Journal of the Technical University of Gabrovo

https://mc04.manuscriptcentral.com/jtug

EFFECT OF THE INFILL ARCHITECTURE ON THE MECHANICAL PROPERTIES OF 3D PRINTED PETG SAMPLES

Nikolay Petrov[1*], Maria Ormanova[1,2,3], Iliya Zhelezarov[1,3]

[1] *Technical University of Gabrovo, 5300 Gabrovo, Bulgaria*

[2] *Institute of Electronics of Bulgarian Academy of Sciences, 1784 Sofia, Bulgaria*

[3] *Center of Competence "Smart Mechatronic, Eco-and Energy-Saving Systems and Technologies", 5300 Gabrovo, Bulgaria*

ARTICLE INFO

Article history:
Received 17 October 2025
Revised 4 November 2025
Accepted 7 November 2025

Keywords:
3D printing, PETG, infill architecture, tensile properties, flexural properties

http://doi.org/10.62853/HHVS3786

ABSTRACT

In the present work, polyethylene terephthalate glycol (PETG) tensile and flexural test specimens were fabricated using the fused filament fabrication (FFF) technique. The samples had different infill densities, namely 35% and 100%, and different infill layer architectures – 45° and 90°. Mechanical tests were performed in order to determine the influence of the chosen 3D printing technological conditions on the flexural and tensile strengths of the samples. The results indicated that in all cases increasing the infill density increased the mechanical performance of the specimens. At low infill densities the change in the orientation of the samples had minimal effect on the mechanical capabilities of the samples, however, increasing the infill density to 100% led to a slight increase of the tensile strength and a major increase of the flexural strength.

1. INTRODUCTION

In an era of a new industrial paradigm, namely Industry 4.0 (I40), full automation of the manufacturing process is required [1]. Of course manufacturing processes start to finish are quite complex and require the combination of vast self-sufficient systems that work in complete synch. Often one of those systems employs some sort of additive manufacturing (AM) technology, depending on the desired materials and designs. Additive manufacturing has recently gained popularity due to the possibility of rapid manufacturing of components based on a computer-aided design (CAD) models [2]. This technology is based on the addition of material to a volumetric specimen as compared to traditional methods for manufacturing such as milling. Due to the high accuracy and precision of the AM techniques the production of components for a minimal amount of time, with near zero material losses, and at a low cost is possible [3].

A number of different methods exist that are even today used for the realization of the additive manufacturing process. Based on the materials used for manufacturing they are most commonly divided into two primary categories (although other secondary categories exist) – additive manufacturing setups for the production of metallic components and metallic alloys, and additive manufacturing setups for the production of polymeric components [3, 4]. Components made of metals and alloys are typically produced using techniques based on the so-called direct energy deposition, which involves the application of a direct high-energy heat source, which is used to melt the material and implement it into the bigger structure. Based on the used heat source these techniques are mostly divided into three categories – ones that use lasers, ones that use an electric beam, and ones that use an electric arc as a heat source [5]. Considering polymeric materials two primary methods are used – fused filament fabrication (FFF) and stereolithography (SLA). Stereolithography is based on the use of a molten resin that is hardened under the influence of a laser beam [6]. Typically, this method characterizes with higher accuracy of production and also makes it possible to produce components with more intricate internal geometries compared to FFF. However, fused filament fabrication is much simpler, easer for designers to familiarize with, and also much more cost effective. Modern technological advances have led to the improvement of the accuracy of deposition and the strength of the output components as well [7]. Due to this, as of today, FFF is the more commonly used approach for production of polymeric components. It is based on the insertion of a solid polymeric wire (filament) into a heated extruder nozzle. Influenced by the heat, the filament melts and is fed through the nozzle, where it is applied to the substrate. The FFF process was better explained in more details by the authors of [8].

Typical polymers used for the production of components using the FFF technology are polylactic acid

* Corresponding author. E-mail: nikolaypetrov44@mail.bg

(PLA), polyethylene terephthalate glycol (PETG), acrylonitrile butadiene styrene (ABS), acrylonitrile styrene acrylate (ASA), polyamide (PA), polypropylene (PP), and exotic ones doped with microparticles with aim to improve their chemical and mechanical properties [9-13]. Based on polyethylene (PE), which is one of the most commonly used polymer for the production of packaging, construction materials, everyday household items, etc., polyethylene terephthalate (PET) was created. The latter, however, despite exhibiting excellent chemical resistance and great mechanical strength, proved to be too brittle to use for the production of components using fused filament fabrication. Due to this, it was used as a base to create the widely spread material polyethylene terephthalate glycol (PETG) by means of addition of the glycol modifier 1.4-cyclohexanedimethanol (CHDM). PETG also has great chemical resistivity and mechanical strength with the addition of great plasticity, and a lower melting temperature [14].

Current advances of 3D printing PETG components using the FFF technique show some of the correlations between the technological conditions of deposition versus the output characteristics of the components. Previous investigations show the relationship between the infill density, infill geometry, layer thickness, and printing temperature and the resultant mechanical properties of the specimens [15, 16]. However, the influence of the infill architecture is still quite unknown. Very little information is present at the current moment regarding that topic. Furthermore, it is still unknown whether, or rather to what extent, would the infill architecture influence the mechanical properties of PETG components at different infill densities.

Due to this in the present work PETG tensile and flexural test components were produced using fused filament fabrication. Two different infill densities and two different infill architectures were employed in order to show the correlation between structure and mechanical strength. The results were discussed in relation to the further optimization of the manufacturing process.

2. EXPERIMENTAL PART

For the purpose of this work the samples were prepared using the fused filament fabrication (FFF) technique. A schematic of the latter is shown in Fig. 1. The desired material is pulled through a small nozzle with a diameter of 0.4 mm by a system of mechanical rollers. The head of the extruder is heated to a temperature, higher than the temperature of melting of the polymeric material, and the last is applied atop the surface of the substrate. The subsequent layers are applied on top of the previously deposited ones by mean of partial re-melting of the latter. The head of the printed, used for deposition of the material has three degrees of freedom – along the x, y, and z axis. The 3D model of the samples was designed using a CAD software, namely SolidWorks 2013, and using the manufacturer's pre-made slicer the model is transferred to the printer in the form of a G-code file.

The technological conditions and some specifics of the printing process are summarized in Table 1. The temperature of the nozzle T_D was 240°C, the temperature of the print bed T_{BED} was 80°C, and the print speed v_D was 300 mm/s. Four initial layers of 100 % infill density are applied on all external parts of the built samples, as shown in Fig. 2a. These conditions remained constant throughout the experiments. In all cases, the orientation of the infill was varied between 45° and 90°, as shown in Fig. 2b,c and Fig. 2d,e, correspondingly. Additionally, two different sets of infill densities were tested, namely 35 % and 100 %. Samples S1-S2 were produced using 35 % infill density, and samples S3-S4 were produced using 100 % infill density. The print time and the material used varied depending on the orientation of the pattern, but mostly as a function of the infill density. The average print time between samples S1-S2 was about 18 minutes, and in the case of samples S3-S4 it was about 28 minutes. Evidently, with the increase of the input material the cost for production increased as well. Interestingly with the increase of the infill density with 65 %, the print time, the material used and the cost increased as well by exactly the same amount.

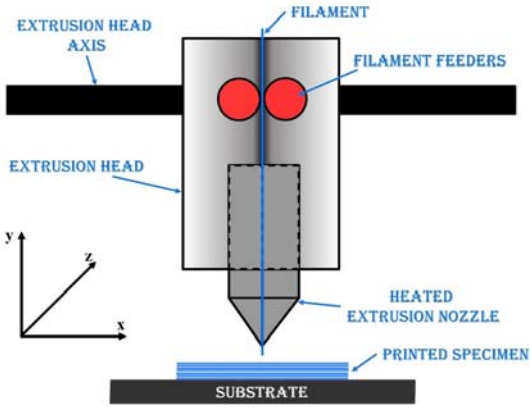

Fig. 1. Schematic of the fused filament fabrication (FFF) process

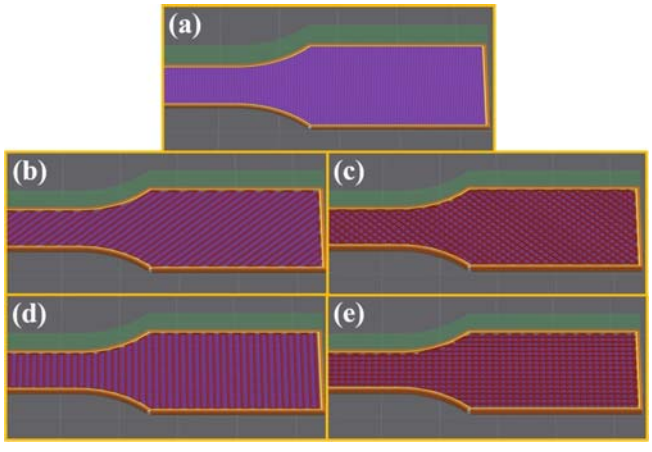

Fig. 2. Initial infill pattern orientation (a), 45° infill pattern orientation (b)-(c), and 90° infill pattern orientation (d)-(e), at 35% density

Table 1 *Technological conditions of printing, print time, material used, and material cost*

Sample	*T_D, °C*	*T_{BED}, °C*	*V_D, mm/s*	*Layer orientation*	*Infill density*	*Print time*	*Material used, g*	*Material cost, €*
S1	*240*	*80*	*300*	*45°*	*35%*	*18m50s*	*9.11*	*0.1822*
S2	*240*	*80*	*300*	*90°*	*35%*	*17m59s*	*8.96*	*0.1792*
S3	*240*	*80*	*300*	*45°*	*100%*	*29m55s*	*14.17*	*0.2834*
S4	*240*	*80*	*300*	*90°*	*100%*	*28m02s*	*14.21*	*0.2841*

The geometry and dimensions of the tensile test samples are shown in Fig. 3. They were selected in agreement with the ISO 527-1:2019 [17] standard for tensile testing of polymeric materials. The length of the samples was 170 mm, the length of the work area was 86 mm, the thickness of the work area was 10 mm, and the thickness of the sample was 5 mm. A ZwickRoell Vibrophore 100 unit was used for all experiments. A static strain mode was employed with a pre-load force of 0.1 MPa, and a test speed of 50 mm/min.

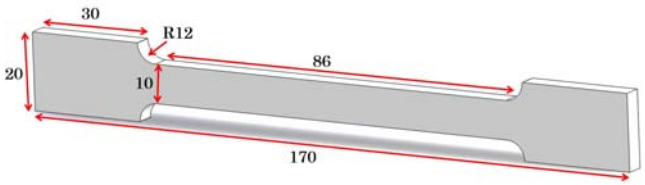

Fig. 3. 3D Printed tensile test sample dimensions

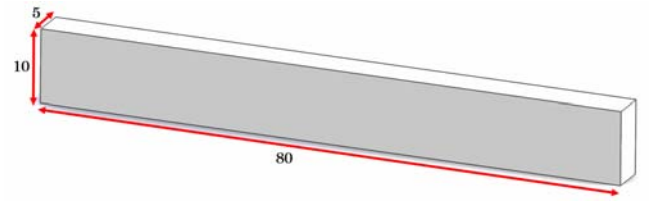

Fig. 4. Flexural test samples dimensions

The ZwickRoell Vibrophore 100 unit was used again for the flexural tests, following the ISO178:2019 standard for flexural testing of polymeric materials [18]. A pre-load of 0.1 MPa was used in all cases with a test speed of 1 mm/min. The geometry and the dimensions of the samples used for the flexural tests are shown in Fig. 4. The length of the samples was 80 mm, the width 10 mm, and the thickness 5 mm. The distance between the anvils was 30 mm.

3. RESULTS AND DISCUSSION

Figure 5a shows an optical image of the macrostructure of the samples prepared using a 45° layer orientation. Similarly, figure 5b shows the macrostructure of the samples prepared using a 90° layer orientation. In all cases, the layers are evenly thick without major defects present in the structure caused by printing errors or poor adhesion. Some mild irregularity was observed in the case of applying layers at a 45° angle where the layers seem slightly bent and not perfectly parallel. This, however, could also be an optical effect due to the angle of the sample positioned on the microscope's specimen stage.

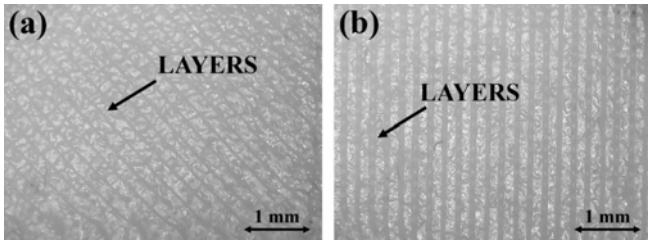

Fig. 5. Optical images of the layers applied using a 45° (a) and 90° (b) orientation

The results of the tensile tests and the flexural tests are listed in Table 2. Looking at the numbers comparatively the lowest tensile strength of 17.7 MPa was obtained using a 90° layer printing orientation at 35% infill density. The highest was that of the sample prepared using a 90° orientation of printing at 100% infill density. The same tendency was observed when investigating the flexural properties of the samples. The ones built using the 90° layer orientation have the biggest discrepancy of the results. In the case of having infill density of 35%, the lowest flexural strength of 28.4 MPa was observed, and in the case of having an infill density of 100%, the highest flexural strength of 39.9 MPa was obtained.

Table 2 *Tensile and flexural test results of all samples*

Sample	***Tensile tests***		***Flexural tests***	
	R_m, *MPa*	ε_m, *%*	σ_f, *MPa*	ε_f, *%*
S1	*19.4 ±1.0*	*1.9 ±0.1*	*29.3 ±1.4*	*9.2 ±0.5*
S2	*17.7 ±0.9*	*1.8 ±0.2*	*28.4 ±1.4*	*8.3 ±0.4*
S3	*32.3 ±1.2*	*2.0 ±0.4*	*30.5 ±1.6*	*13.1 ±0.6*
S4	*33.7 ±1.3*	*1.7 ±0.1*	*39.9 ±1.5*	*8.9 ±0.5*

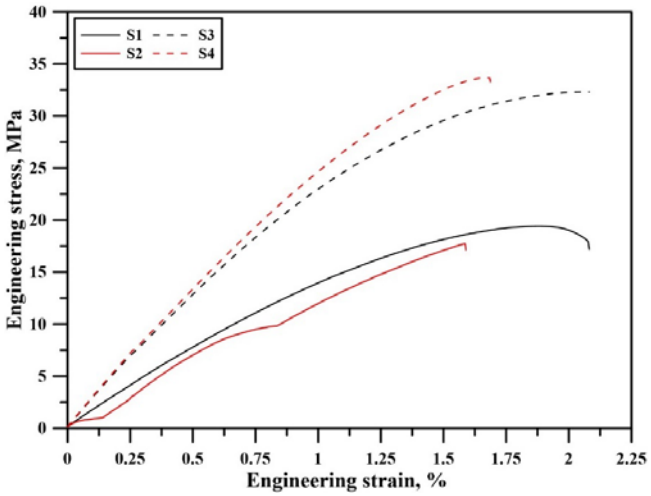

Fig. 6. Tensile test stress-strain curves of samples S1-S4

Figure 6 shows the stress-strain curves of all samples obtained during the tensile tests. Comparing samples S1 and S2 although the angle of the curves is approximately the same, in the case of sample S2 a sudden drop is observed, followed by a subsequent recovery of the relationship between stress and strain. The sudden drop in the curve probably occurred due to one of two reasons. Either there was a short misfunction of the testing unit causing errors in the data, or more probably there was a fail of some of the polymeric strands that the sample is made of. Considering samples S3 and S4 in both cases the maximum stress values are higher. No abnormalities were observed in the characteristic of the curves. All tested samples exhibited a very low level of elongation (about 2 %), which means that the samples fail suddenly without warning. Although this is typical for PETG samples [19], this is undesirable in some constructions where the material is expected to have some give prior to complete failure [20].

Figure 7 shows the strain-stress curves obtained during the flexural test experiments. In the case of samples S1 and S2 the permanent plastic bending of the samples occurred at approximately the same flexural stress value, however, the further response of the samples was different. The plastic deformation of sample S2 was much faster and required less force. This means that using a 90° layer orientation weakened the structure of the samples at the lower infill

density. Interestingly, when increasing the infill density to 100 % a vastly different result was observed. In the case of the sample (S3) prepared at 45° orientation of the infill pattern the permanent plastic deformation occurred at lower levels of flexural stress. Subsequently, the increase of the deformation of the samples was linear and advanced at the same value of the applied force. Considering sample S4 a much higher flexural strength value was obtained with the force required for further deformation exhibiting a declining character.

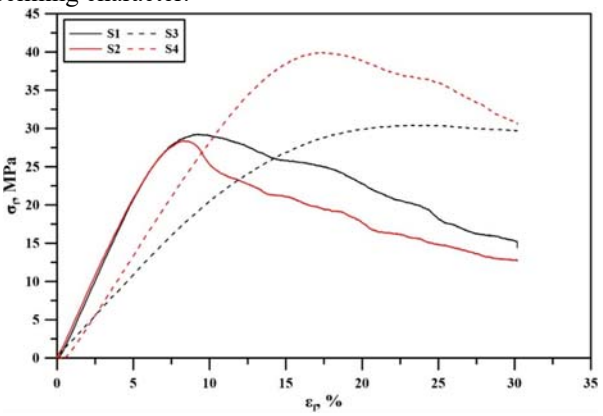

Fig. 7. Flexural test stress-strain curves of samples S1-S4

The fracture zones of the tensile test samples after the performed experiments are shown in figure 8. Samples S1 and S2 are shown in figures 8a, and 8b, correspondingly. Samples S3 and S4 are shown in figures 8c, and 8d, accordingly. A noticeable discrepancy was observed previously where sample S2 showed the lowest tensile strength. Due to the low density of the infill of the samples major voids are seen that are perfectly perpendicular to the applied tensile force. In the case of sample S1 at the same density the applied layers are diagonal of the applied tensile force, which increased the strength of the samples. Increasing the infill density to 100 %, however, led to a major increase of the tensile strength of the samples, particularly of that built using a 90° infill layer orientation. The high density negated the orientation of the layers. Not only that, but the more orderly nature of the 90° infill pattern increased the density of the samples and resulted in a more uniform distribution of the tensile force. Studying sample S4 some adhesion layer failures are visible, however, they did not substantially affect the maximum tensile force of this sample.

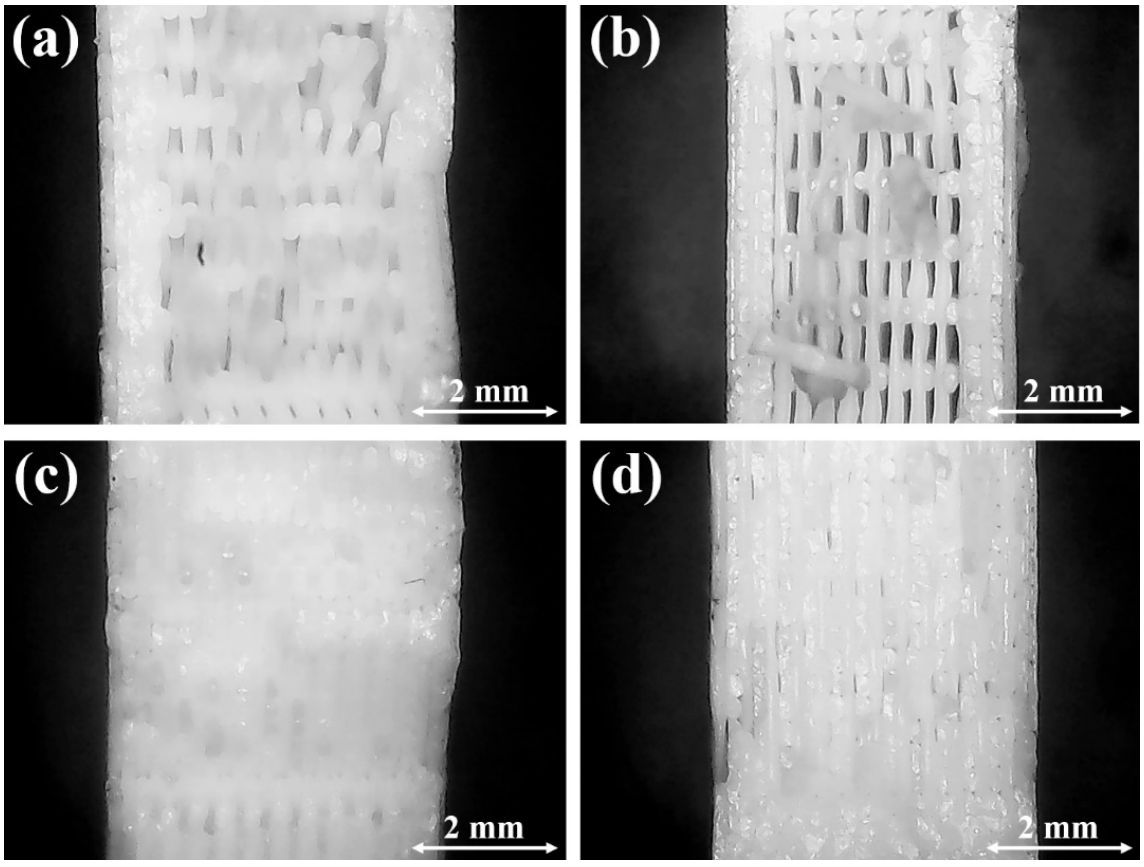

Fig. 8. Optical images of the fracture zone of the tensile test samples (a) S1, (b) S2, (c) S3, and (d) S4

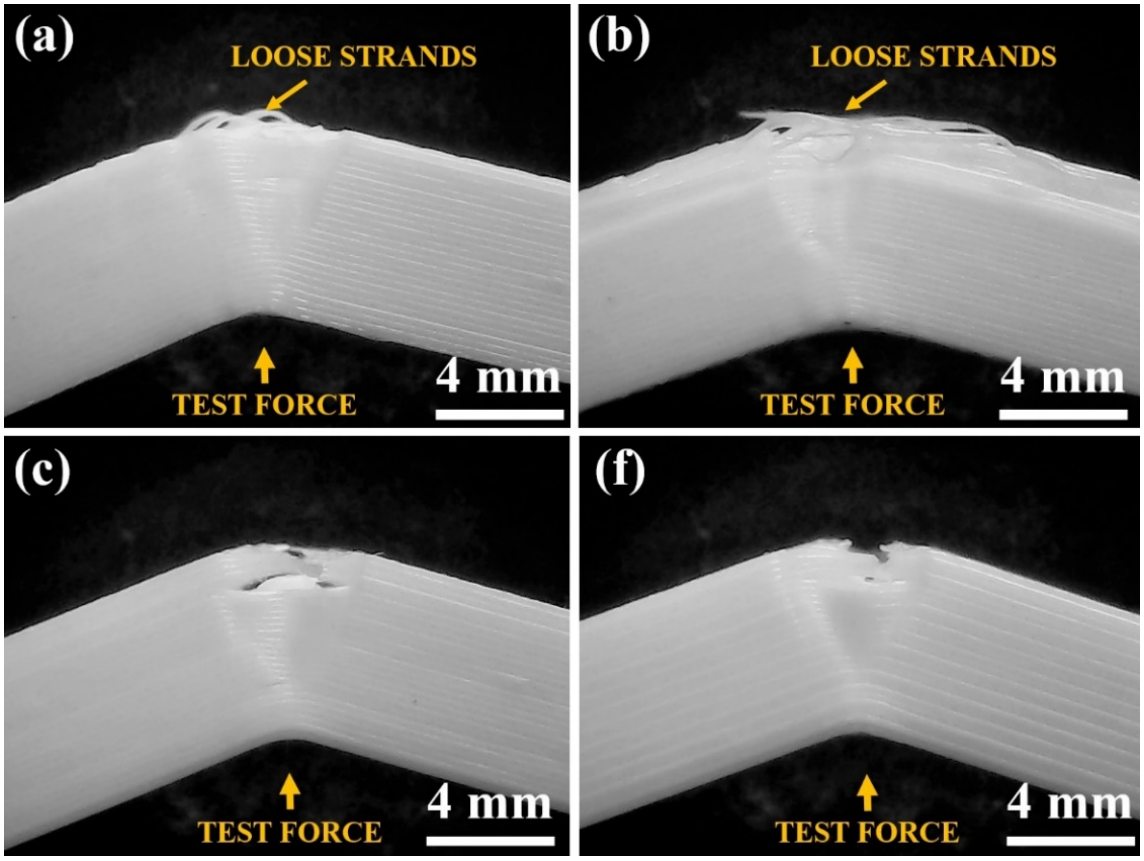

Fig. 9. Optical images of the bent zone of the flexural test samples (a) S1, (b) S2, (c) S3, and (d) S4

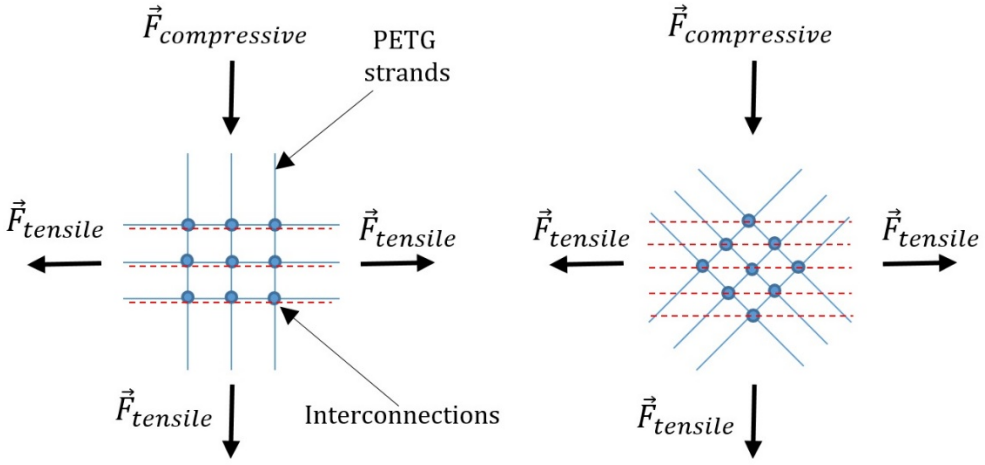

Fig. 10. Cross-joints formed during the building of PETG components using (a) a 90° layer orientation and (b) a 45° orientation of the layers

Figure 9 shows images of the flexural test samples after the performed experiments. In figures 9a and 9b samples S1 and S2 are shown, accordingly. In Fig. 9c and 9d samples S3 and S4 are shown. Due to the lower density of the samples prepared using 35% infill density, loose strands can be seen at the bottom of the flexural samples. This weakened the structure of the latter and reduced their mechanical performance. In the case of the samples prepared using 100% infill density, no loose strands were observed. Although some adhesion problems between internal layers were noticed in the tensile test samples, no signs of such defects were visible in the flexural test samples.

During the experiments a noticeable trend was observed where in the case of a lower density of the samples (35%) the ones prepared with layers at a 45° angle had better mechanical properties in all cases compared to the ones prepared with layers at 90°. The exact opposite trend was observed by increasing the density of the samples to 100%. Figure 10 shows a basic representation of the cross-joints formed by interconnecting the separate layers at both the 90° orientation of the layers (Fig. 10a) and at 45° orientation of the layers (Fig. 10b). Based on the orientation of the layers a different concentration of the joints is formed as a function of their position in the samples. As a result, higher density of the joints is observed at 45° compared to 90° at 35% infill density. This increases the strength of the samples, meaning that at lower densities it is preferable to build PETG components using fused filament fabrication at 45° orientation of the layers. Changing the infill density to 100 % negates the necessity of the 45° orientation, and not only that, but due to the better

symmetry of the 90° orientated layers more interconnected joints form in that case. Due to this, the mechanical properties of the samples improved in all cases. Also this slightly improves the isotropic properties of the samples. Based on the performed experiments it can be concluded that a 90° orientation of the layers is preferable when building PETG components at high infill densities. More experiments need to be performed to determine the exact point where the 90° orientation becomes more favorable.

PETG is a polymer that possessed excellent properties. It has high chemical resistivity and good mechanical strength. A tensile strength of 60-80 MPa of standard build PETG components is typical for this material. It also exhibits great thermal resistance. Due to this, it is not uncommon to be the material of choice for: scaffoldings in tissue engineering; drug containers; dental implants; orthopedic applications; and others [21]. However, as mentioned the desired strength of the components needs to be substantially higher compared to the obtained not only in this research, but in other previous ones [22] using 3D printing. This imposes the need for improvement of the technological conditions during 3D printing, particularly using fused filament fabrication, in order to improve the quality of the components and expand their applicability. There are of course other applications such as in the food or electronic industries where the mechanical strength of the build components is not a focus for designers, as opposed to other properties such as the already mentioned thermal resistance, chemical resistance, electrical isolating properties [23] or in the case of incorporating carbon particles within the PETG matrix electrical conductivity [24], and more. Additionally, PETG components with similar strength have been tested in cryogenic conditions of up to -196°C and the effect of that treatment was discussed by Stan et al. [25].

4. CONCLUSION

The results of the presented work can be summarized with the following conclusions:

1. The increase of the infill density from 35% to 100% led to an increase of the mechanical properties of the samples in all cases;

2. At low infill densities the application of a 90° infill architecture led to a reduction of the tensile and flexural strengths of the samples;

3. At high infill densities the application of a 90° infill architecture led to an increase of the tensile strength and the flexural strength of the samples;

4. A 90° infill layer architecture at low infill densities contains a substantial amount of voids which reduced the adhesion between the layers and increased the applied stress on key areas of the samples where their walls were the thinnest;

5. Increasing the infill density negated the formation of voids and increased the density and adhesion of the samples more than those of the samples prepared at 45° infill density orientation.

This work shows the correlation between the infill density and the infill layer orientation and their influence on the mechanical properties of the studied samples. Despite the expected linearity of the results, the actual ones show that the correlation changes depending of the architecture of the samples. This emphasizes the importance of properly selecting the correct printing conditions necessary for successful implementation of the produced components.

REFERENCES

[1] Bortolini M., Ferrari E., Gamber M., Pilati F., Faccio M., Assembly system design in the Industry 4.0 era: a general framework, IFAC PapersOnLine 50 (2017) 5700–5705

[2] Wong K., Gernandez A., A Review of Additive Manufacturing, International Scholarly Research Notices (2012) 208760

[3] Frazier W., Metal Additive Manufacturing: A Review, Journal of Materials Engineering and Performance 23 (2014) 1917–1928

[4] Jafferson J., Chatterjee D., A review on polymeric materials in additive manufacturing, Materials Today: Proceedings 46 (2021) 1349–1365

[5] Vafadar A., Guzzomi F., Rassau A., Hayward K., Advances in Metal Additive Manufacturing: A Review of Common Processes, Industrial Applications, and Current Challenges, Applied Science 11 (2021) 1213

[6] Manapat J., Chen Q., Ye P., Advincula R., 3D Printing of Polymer Nanocomposites via Stereolithography, Macromolecular Materials and Engineering 302 (2017) 1600553

[7] Pazhamannil R., Jishnu N., Govindan P., Abhilash E., Property enhancement approaches of fused filament fabrication technology: A review, Polymer Engineering and Science 62 (2022) 1356–1376

[8] Rashid A., Koc M., Fused Filament Fabrication Process: A Review of Numerical Simulation Techniques, Polymers 13 (2021) 3534

[9] Irshadullah Wasif M., Ftima A., Tufail M., Accurate additively manufactured PETG molds for the composite manufacturing, Proceedings of Researchfora International Conference, Istanbul, Turkey (2023) 6–8

[10] Aumnate C., Pongwisuthiruchte A., Pattananuwat P., Potiyaraj P., Fabrication of ABS/Graphene Oxide Composite Filament for Fused Filament Fabrication (FFF) 3D Printing, Advances in Materials Science and Engineering (2018) 2830437

[11] Cojocaru V., Frunzaverde D., Miclosina C., Marginean G., The Influence of the Process Parameters on the Mechanical Properties of PLA Specimens Produced by Fused Filament Fabrication - A Review, Polymers 14 (2022) 886

[12] Rakshit R., Kalvettukaran P., Acharyya S., Panja S., Misra D., Development of high specific strength acrylonitrile styrene acrylate (ASA) structure using fused filament fabrication, Progress in Additive Manufacturing 8 (2023) 1543–1553

[13] Casamento F., Padovano E., Pappalardo S., Frache A., Badini C., Development of polypropylene-based composites through fused filament fabrication: The effect of carbon-based fillers, Composites, Part A: Applied Science and Manufacturing 164 (2023) 107308

[14] Zhang Z., Yao Z., He Y., Yu S., Chen M., Shi Z., He J., Xiang H., Zhu N., Melt-spun poly (ethylene terephthalate-co-1,4-cyclohexanedimethylene terephthalate) (PETG) copolyester fibers: Synergistic effect of chemical and crystal structure regulation, Polymer Engineering and Science 65 (2025) 755–764

[15] Kadhum A., Al-Zubaidi S., Abdulkareem S., Effect of the Infill Patterns on the Mechanical and Surface Characteristics of 3D Printing of PLA, PLA+ and PETG Materials, ChemEngineering 7 (2023) 46

[16] Srinivasan R., Ruban W., Deepanraj A., Bhuvanesh R., Bhuvanesh T., Effect on infill density on mechanical properties of PETG part fabricated by fused deposition modeling, Materials Today: Proceedings 27 (2020) 1838–1842

[17] ISO 527-1:2019 Plastics – Determination of tensile properties, ISO: Geneva, Switzerland, 2019

[18] ISO 178:2019 Plastics – Determination of flexural properties, ISO: Geneva, Switzerland, 2019

[19] Dohan V., Galatanu S., Marsavina L., Mechanical evaluation of recycled PETG filament for 3D printing, Fracture and Structural Integrity 70 (2024) 310–321

[20] Boyd M., Navy Department Advisory Committee on Structural Steel, In Brittle Fracture in Steel Structures, Butterworth & Co., London, UK (1970)

[21] Yan C., Kleiner C., Tabigue A., Shah V., Sacks G., Shah D., DeStefano V., PETG: Applications in Modern Medicine, Engineered Regeneration 5 (2024) 45–55

[22] Hsueh M., Lai C., Wang S., Zeng Y., Hsieh C., Pan C., Huang W., Effect of Printing Parameters on the Thermal and Mechanical Properties of 3D-Printed PLA and PETG, Using Fused Deposition Modeling, Polymers 13 (2021) 1758

[23] Sepahi M., Abusalma H., Jovanovic V., Eisazadeh H., Mechanical Properties of 3D-Printed Parts Made of Polyethylene Terephthalate Glycol, Journal of Materials Engineering and Performance 30 (2021) 6851–6861

[24] Alhat S., Yadav M., Mechanical and Electrical Behavior of Polyethylene Terephthalate Glycol (PETG) Reinforced with Multiwall Carbon Nanotubes (MWCNT) by using Fused Deposition Modeling 3D Printing, International Research Journal of Engineering and Technology (IRJET) 7 (2020) 1405–1413

[25] Stan F., Stanciu N., Sandu I., Fetecau C., Serban A., Effect of low and extreme-low temperature on mechanical properties of 3D-Printed polyethylene terephthalate glycol, The Romanian Journal of Technical Sciences, Applied Mechanics 64 (2019) 21–41